

Global motion integration in the cat's lateral posterior-pulvinar complex

Daniela Dumbrava, Jocelyn Faubert and Christian Casanova

École d'optométrie, and Centre de recherche en sciences neurologiques, Université de Montréal, CP 6128, succ. Centre-ville, Montréal, Québec, Canada H3C 3J7

Keywords: complex motion, cortico-thalamo-cortical loops, extrageniculate thalamus, higher-order processing, spatio-temporal integration

Abstract

Our laboratory previously showed that thalamic neurons in an extrageniculate nucleus, the lateral posterior-pulvinar complex (LP-pulvinar) could perform higher-order neuronal operations that had until then only been attributed to higher-level cortical areas. To further assess the role of the thalamus in the analysis of complex percepts, we have investigated whether neurons in the LP-pulvinar complex can signal the direction of motion of random-dot kinematograms wherein the individual elements of the pattern do not provide coherent motion cues. Our results indicate that a subset of LP-pulvinar cells can integrate the displacement of individual elements into a global motion percept and that their large receptive fields permit the integration of motion for elements separated by large spatial intervals. We also found that almost all of the global motion-sensitive neurons were not systematically pattern-motion-selective when tested with plaid patterns. The results indicate that LP-pulvinar cells can perform the higher-level spatio-temporal integration required to detect the global displacement of objects in a complex visual scene, further supporting the notion that extrageniculate thalamic cells are involved in higher-order motion processing. Furthermore, these results provide some evidence that there may be specialized mechanisms for processing different types of complex motion within the LP-pulvinar complex.

Introduction

Visual scenes often contain many elements moving in various directions that need to be combined to yield a global and coherent motion percept. On the basis of psychophysical and electrophysiological evidence, it has been suggested that motion integration occurs in at least two stages (Adelson & Movshon, 1982; Watamaniuk *et al.*, 1989; Stoner & Albright, 1992). The first stage, likely to take place in the primary visual cortex, would extract the local motion characteristics of an image. However, the individual local motion signals encoded at this first stage are often inherently ambiguous because of the restricted spatial extent of the receptive fields of first-order neurons (the aperture problem; see Adelson & Movshon, 1982.). This problem can be resolved at a second stage that combines the locally measured signals over space and time to form a globally coherent motion percept. This second level of analysis is believed to take place in higher-order visual cortical areas such as the middle temporal (MT) area in primates (Movshon *et al.*, 1985; Rodman & Albright, 1989) and the anterior ectosylvian visual (AEV) cortex in cats (Scannel *et al.*, 1996).

Our laboratory has recently reported that neurons in the main extrageniculate structure of the visual thalamus, the lateral posterior-pulvinar (LP-pulvinar) complex, can signal the veridical direction of motion of a plaid pattern (Merabet *et al.*, 1998), thereby indicating that these neurons can integrate two ambiguous local motion signals into a coherent moving percept. In addition, we demonstrated that

these cells are functionally linked to the AEV cortex, which is the only cortical area in cats known to carry out such integrative neuronal operations (Scannel *et al.*, 1996). These findings support the hypothesis that the thalamus is involved in higher-order functions that were, until recently, only associated with cortical areas beyond the primary visual cortex. The finding that LP-pulvinar cells can perform higher-order motion integration is thus of fundamental importance in the renewed efforts of several laboratories to assess the contribution of the thalamus to higher-level functions using theoretical and experimental means (Mumford, 1991; Miller, 1996; Sherman & Guillery, 1996). To further examine the role of thalamic nuclei in complex sensory processing, we have investigated whether or not LP-pulvinar neurons can signal the global displacement of a random dot kinematogram wherein comprising elements do not provide any local coherent motion cues. The coding of the direction of motion of such patterns by LP-pulvinar neurons would indicate that their receptive fields could perform the higher-level spatio-temporal integration necessary to detect the global displacement of objects in a visual scene.

Materials and methods

General procedures

Cats were preanaesthetized with acepromazine (1 mg/kg body weight) and atropine (0.1 mg/kg). General anaesthesia was carried out using a gaseous mixture of halothane (1–3%) and N₂O/O₂ (50/50%). Animals were treated in accordance with the guidelines of the Canadian Council for the Protection of Animals. All surgical wounds

Correspondence: Dr Christian Casanova, Laboratoire des Neurosciences de la Vision, École d'optométrie, as above.
E-mail: christian.casanova@umontreal.ca

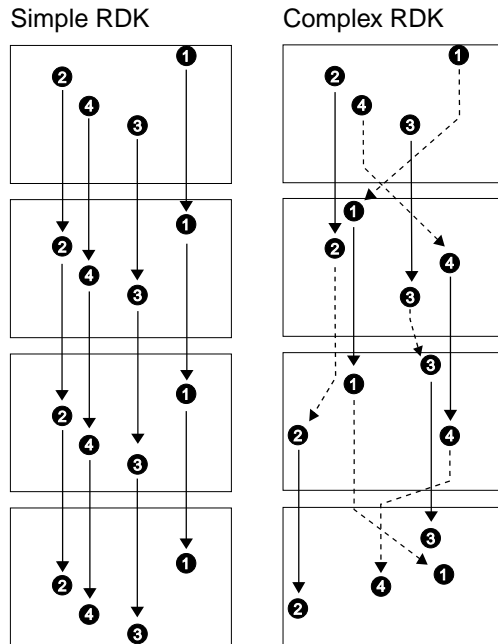


FIG. 1. Schematic of the simple and complex RDKs. Solid lines represent motion signals whilst broken lines illustrate the random repositioning of the corresponding dot. Each rectangle equals one stimulus frame.

and pressure points were infused by a local anaesthetic (lidocaine hydrochloride 2%). Heart rate and O_2 blood saturation were constantly monitored with an oxymeter (Nonin). A cannulation of the right cephalic vein and a tracheotomy were performed. Deep tendon reflexes were checked to ensure a satisfactory level of anaesthesia during the surgery. The cat was then placed in a stereotaxic frame and was paralysed by intravenous injection of gallamine triethiodide (10 mg/kg/h) and artificially ventilated ($N_2O : O_2$: 70% : 30% plus halothane 0.5–1%). Core temperature, electrocardiogram and electroencephalogram were continuously monitored. Pupils were dilated with atropine and nictitating membranes were retracted with local application of phenylephrine hydrochloride (2.5%). The eyes were protected using contact lenses of appropriate refractive power. A craniotomy was performed over the LP-pulvinar complex and the dura was retracted. The exposed cortex was covered with warm agar on which melted wax was applied to create a sealed chamber.

Recordings and visual stimulation

Varnished tungsten microelectrodes were used to record single-unit activity in LP-pulvinar cells. The electrodes were placed after the mapping of the visual field represented in the lateral geniculate nucleus (at two or three distinct coordinates) to verify the precision of stereotaxic adjustments. Neuronal activity was amplified, displayed on an oscilloscope, and played through an audio monitor. A window discriminator was used to isolate single units from the overall signal and waveforms of the action potentials were routinely examined. Digital signals were then fed to an acquisition software (spike2, CED, Cambridge, UK) via an analogue–digital interface (CED 1401 plus). The response for each stimulus condition was recorded as peristimulus time histograms (PSTH) and interspike interval (ISI) histograms (binwidths of 10 ms and 1 ms, respectively) and was saved for further statistical analysis.

Visual stimuli were generated by a Macintosh G3 computer and were back-projected by a LCD projector (InFocus Systems, frame rate of 67 Hz) on a screen subtending $80 \times 107^\circ$ of visual angle placed 57 cm in front of the animal. The screen (Da-Lite, Warsaw, IN, USA) was made of a precise optical coating applied to an acrylic substrate (Da-Plex) permitting a display of high optical quality and a uniform diffusion of the light projected onto it. Receptive fields were first characterized by presenting drifting sinusoidal gratings. Then, random-dot kinematograms (RDKs) consisting of white dots (100% contrast) on a black background were used to study global motion processing. Two stimuli were used to differentially emphasize global motion mechanisms. For convenience, these will be referred to as simple and complex RDKs (Fig. 1). The simple RDK (Fig. 1A) was essentially a sequence of *phi* motions (apparent motion perceived when two dots flicker in alternation) that included motion energy and only required minimal simultaneous motion integration over an area of the visual field. In this configuration, each dot followed a straight and continuous path, always at the same velocity. The dot lifetime was equal to that of presentation time (no repositioning), and the display was a rigidly translating random dot field with no noise. For complex RDKs (Fig. 1B), the dots had a lifetime of two frames (16–64 ms depending on test conditions), that is, they moved only once before being randomly repositioned (displaced to another spatial location). Over a temporal sequence of a given set of displacements, 100% of the dots contributed to the global motion sequence. Each dot had an equal random probability of beginning at the first or second frame of their motion sequence. In this stimulus, half of the dots were displaced in the motion direction while the remaining half were repositioned randomly (Fig. 1). In other words, the signal and noise frames were segmented by half on any given frame presentation so that when half of the dots give the motion signals the remaining ones repositioned themselves (the reverse being observed in the next sequence). This configuration is similar to the ‘Combined condition’ described by Williams & Sekuler (1984). In the complex RDK, there is never more than a single *phi* motion jump before repositioning. Consequently, there must be spatial and temporal integration of the dots’ displacement over an extended area of the visual field in order to signal the veridical direction of the pattern. Computing the following index compares response strength to both stimuli: mean response to complex RDKs at optimal direction (MRC)/mean response to simple RDKs at optimal direction (MRS). A MRC/MRS value < 1 would indicate that responses to simple RDKs are more robust than those to complex RDKs.

Varying the spatial (D) and temporal (T) intervals at which the dots were plotted allowed for the control of the perceived velocity of the motion stimulus. The maximum displacement within which a cell still preferred a direction of motion of the pattern (D_{max}) was also determined for a subset of neurons. The dot diameter was varied between 0.1 and 1° of visual angle and in most cases, given the large size of LP-pulvinar receptive fields, the optimal responses were obtained for 1° dots. The presentation time was 4 s for both types of motion. The interframe interval was always equal to the frame duration. Stimuli were presented for at least four complete trials consisting of 12 interleaved directions of motion in 30° increments. For a subset of cells, responses to drifting plaids were studied. Plaids were generated by a frame-interleaved method and were composed of two superimposed sine-wave gratings differing in orientation (120°) but of identical spatial frequency, temporal frequency and contrast. Responses to plaids were classified as pattern motion (PM)- or component motion (CM)-selective by calculating partial correlations using the following formula: $R_p = (r_p - r_c r_{pc}) / [(1 - r_c^2)(1 - r_{pc}^2)]^{1/2}$ (Movshon *et al.*, 1985; corrected). R_p represents the partial correlation coefficient for the pattern prediction, r_c is the correlation coefficient of

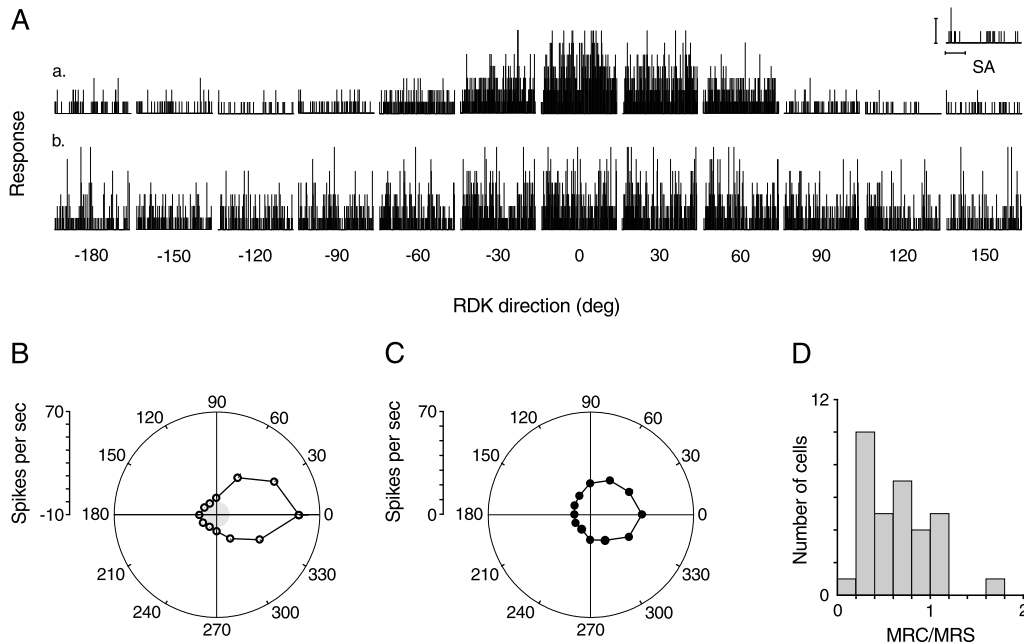


FIG. 2. Responses of an LP-pulvinar neuron to (Aa) simple and (Ab) complex RDKs shown as PSTHs (SA, spontaneous activity); (B) and (C), respectively, corresponding tuning curves. SEM bars are too small to be visible. Note that the response to the complex RDK is less robust and less sustained than that of the simple RDK. (D) The distribution of the strength index for all complex RDK-selective cells. In panel B, data points within the shaded region represent cell discharges below spontaneous activity levels. Scale bars in panel A (inset) are 2 spikes/bin (vertical) and 1 s (horizontal).

the plaid response calculated from the component model, r_p is the correlation coefficient for the plaid response from the pattern model, and r_{pc} is the correlation coefficient for the two models. Similarly, R_c is the partial correlation defined for the CM prediction and is calculated by exchanging r_p with r_c in the equation. A cell is considered pattern motion-selective when the value of R_p is significantly greater than either R_c or zero.

For each cell, a direction selectivity index (DI) was calculated using the formula $DI = 1 - N/P$, where N is the mean response in the nonpreferred direction minus spontaneous activity, and P is the mean response in the preferred direction minus spontaneous activity. Cells with a $DI > 0.5$ were considered selective to the direction of the stimulus motion.

Electrolytic lesions were made along each recording track. At the end of each experiment, the animal was killed with an overdose of sodium pentobarbital (Euthanyl, 120 mg/Kg). The brain was removed from the skull and fixed in a solution of buffered formalin (10%). After 5 days, 40–100- μ m serial sections of the brain were cut in the frontal plane. Every third section was stained to reveal acetylcholinesterase (AChE) activity (Koelle & Fridenwald, 1949) in order to distinguish the three major zones in the LP-pulvinar, i.e. the medial and lateral zones of the LP (LPm and LPI), and the pulvinar (Graybiel & Berson, 1980). The remaining sections were stained with cresyl violet and were matched with the AChE sections to locate the lesions and determine the position of the cells recorded in the LP-pulvinar.

Results

General observations

A total of 134 visual cells were recorded in the LP-pulvinar complex. The general properties of the cells were typical of those

previously reported (Chalupa *et al.*, 1983; 1989; Casanova *et al.*, 1989; Chalupa & Abramson, 1989). The majority of cells (89.5%) were orientation selective (mean \pm SD bandwidth, $36.8 \pm 2.32^\circ$) and preferred a given direction of motion of drifting gratings (67.9%). The mean optimal spatial frequency was 0.14 ± 0.01 cycle per degree; the majority of cells (76%) exhibited band-pass tuning functions (mean \pm SD, 2.19 ± 0.12 octaves) and the remaining cells were low-pass.

Global vs. local motion sensitivity

Direction-tuning functions

Out of the 134 neurons, 89 were tested for their sensitivity to simple and complex RDKs. The remaining 45 units were lost before the completion of the tests or their visual discharges were too variable to be analysed with confidence.

Eighty-eight percent (79 out of 89) of the LP-pulvinar cells responded to the motion of simple RDKs, and a subset of those (54 of 79, 68%) was selective to the direction of motion. Almost two-thirds of these direction-selective units (33 out of 54) were also direction selective for complex RDKs. Figure 2 shows the response profiles of a cell to both stimuli. The unit was relatively finely tuned for the simple RDK direction (bandwidth of 41.1°) but responded to a broader range of directions (bandwidth of 96.3°) when stimulated with the complex RDK. In addition, the responses evoked by the simple RDK were more robust and sustained than those observed with the complex RDK (see below). Additional examples of direction tuning curves are shown in Fig. 3. Panel A exemplifies the fact that, for most units, responses to simple RDKs were more robust than those computed from complex RDKs. In Fig. 3B and C, for both stimuli, the cells responded optimally with comparable strength when the pattern was drifted at directions between 60 and 90° . Fig. 3D illustrates

the few cases in which the responses to the complex RDK were more robust than those computed from the simple RDK. In all these examples, direction selectivity was preserved whether simple or complex RDKs were presented. For comparison purposes, we studied the responses of a subset of 14 neurons in area 17. All eight of the simple RDK direction-selective neurons either did not respond to complex RDKs or, as shown in panel F, responded to all directions of motion.

Overall, the mean bandwidth (expressed as the half-width of the tuning curve at half-height) for direction computed from complex RDKs was $75.5 \pm 6.9^\circ$, a value that is significantly greater than that computed from simple RDKs ($57.44 \pm 4.7^\circ$; $t = 2.14$, $P = 0.035$) for these cells. The direction bandwidth distribution of cells responding to both stimuli is shown in Fig. 4.

The 18 remaining units only signaled the direction of simple RDK-defined patterns (see Fig. 3D). Their mean direction tuning was $47.4 \pm 5.3^\circ$, a value not significantly different from that computed

from simple RDKs for neurons responding to both stimuli ($t = 1.31$, $P = 0.19$).

Response profile and strength

In general, mean optimal firing rates were greater for simple RDKs than those for complex RDKs (see Fig. 2A–C and Fig. 3A). The distribution of the strength index (see Materials and methods) is shown in Fig. 2C. Clearly most MRC/MRS values are distributed below 1, indicating that LP-pulvinar cells were generally less responsive to complex RDKs (mean MRC/MRS of 0.65 ± 0.06).

Examination of the PSTHs seemed to reveal that, in general, discharges to simple RDKs were more sustained than those evoked by complex RDKs. In the latter case, it was not unusual to observe the presence of burst discharges separated by silent periods. To verify these qualitative observations, we examined the distribution of ISIs computed from optimal responses to both stimuli (see insets in Fig. 5). To confirm the above postulate, one would expect to find

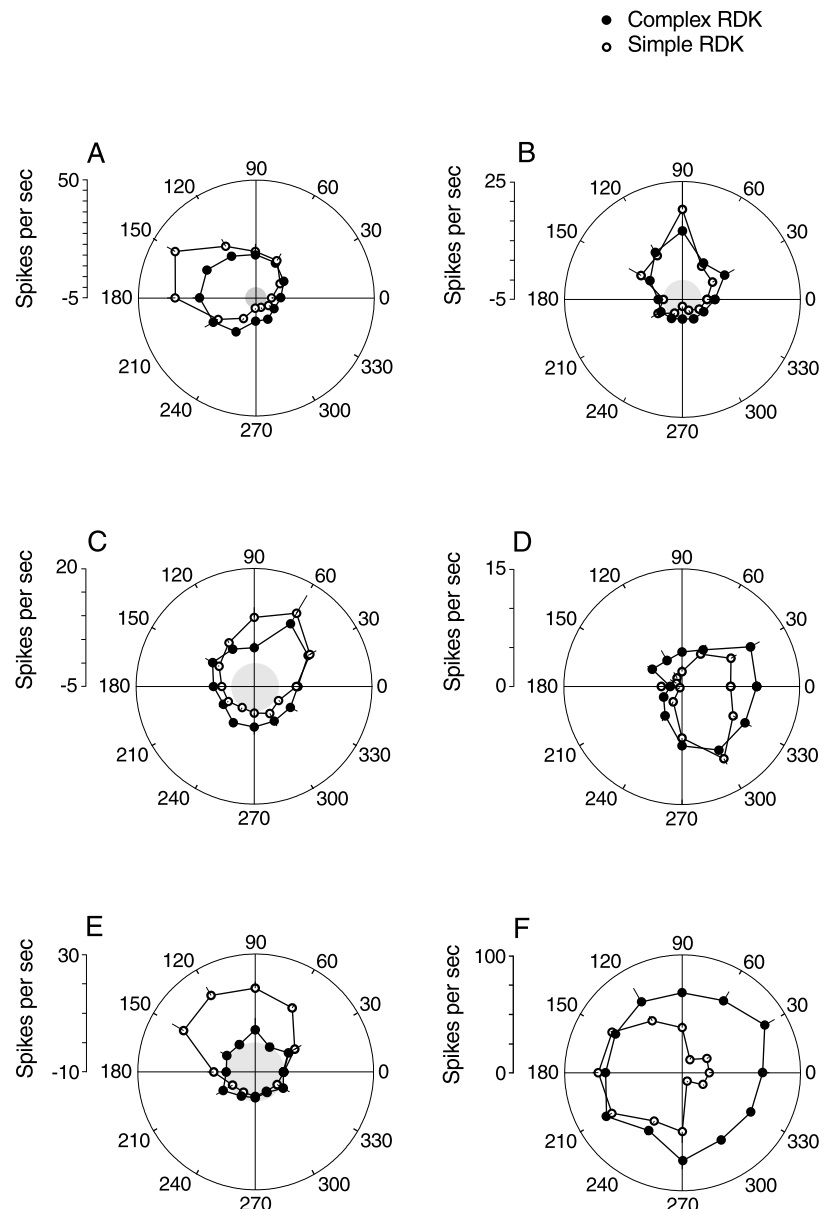


FIG. 3. Polar graphs illustrating the responses of (A–E) LP-pulvinar neurons and of (F) an area 17 cell to simple (empty symbols) and complex (filled symbols) RDKs drifted in 12 directions of motion. (A–D) Examples of complex RDK-sensitive neurons. E presents a cell that only responded to simple RDKs. F shows the RDK responses of a complex cell in area 17. Data points within the shaded regions represent cell discharges below spontaneous activity levels. Element size was 1° except in B and F where it was 0.3° . Bars on data points are SEM.

longer ISIs in the responses to complex RDKs than in the discharges evoked by simple RDKs (Casanova *et al.*, 1995; Merabet *et al.*, 2000). Figure 5 shows the ratio distribution of the number of ISIs between 100 and 400 ms divided by the number of ISIs between 1 and 400 ms. For cells that responded to both stimuli (Fig. 5A and B), the distribution of the ratios is significantly different. The mean ratios are 0.09 ± 0.01 and 0.19 ± 0.02 for simple and complex RDKs ($t = -3.45$, $P < 0.001$) confirming the observation that, when compared to simple RDKs, responses to complex RDKs are less sustained. We also found that response profiles of neurons coding only the motion of simple RDKs tended to differ from the discharges of complex RDK-sensitive units to simple RDKs (compare Fig. 5A and C; means of 0.09 ± 0.01 and 0.16 ± 0.03 , respectively; $t = 2.26$, $P = 0.027$).

Therefore, the LP-pulvinar complex appears to contain two populations of direction-selective neurons. The first one can signal the direction of simple- and complex motion-defined RDKs, and the second can only signal the direction of simple RDKs. We investigated whether the two subsets of cells differ with respect to their general receptive field organization. We found that the mean receptive field size of complex RDK-selective cells (721 ± 61 square degrees) was significantly larger ($t = 3.07$, $P = 0.003$) than the mean of units that only responded to the simple condition (mean 431 ± 47 square degrees). The distribution of receptive field sizes of the two cell groups is shown in Fig. 6A. We also observed differences ($t = 2.52$, $P = 0.015$) for the receptive field location of the two types of cells (Fig. 6B, mean eccentricity of 23.4 ± 3.1 and $18.5 \pm 2.3^\circ$ for global and local motion-selective cells, respectively). For both groups, we did not find any relationship between receptive field size and eccentricity. This may be related to the fact that most receptive fields studied were large and were located more centrally than peripherally. Finally, these two groups of neurons could not be distinguished on the basis of their preference and selectivity for orientation, nor for spatial and temporal frequencies. Of note is the fact that cells responding to complex RDKs tended to exhibit lower preferred spatial frequencies than did neurons that only responded to simple RDKs ($t = -1.75$, $P = 0.08$).

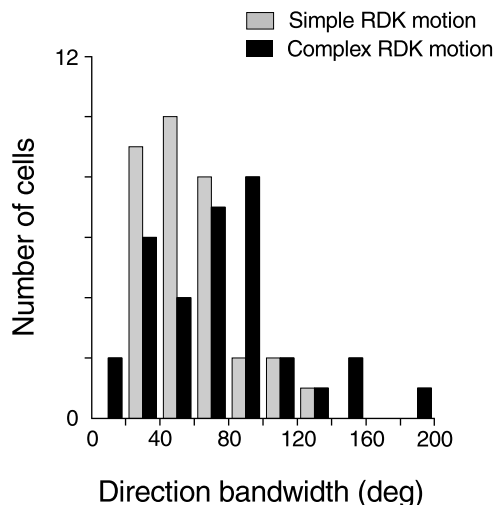


FIG. 4. Distribution of RDK direction bandwidths computed from tuning curves of complex RDK-selective cells.

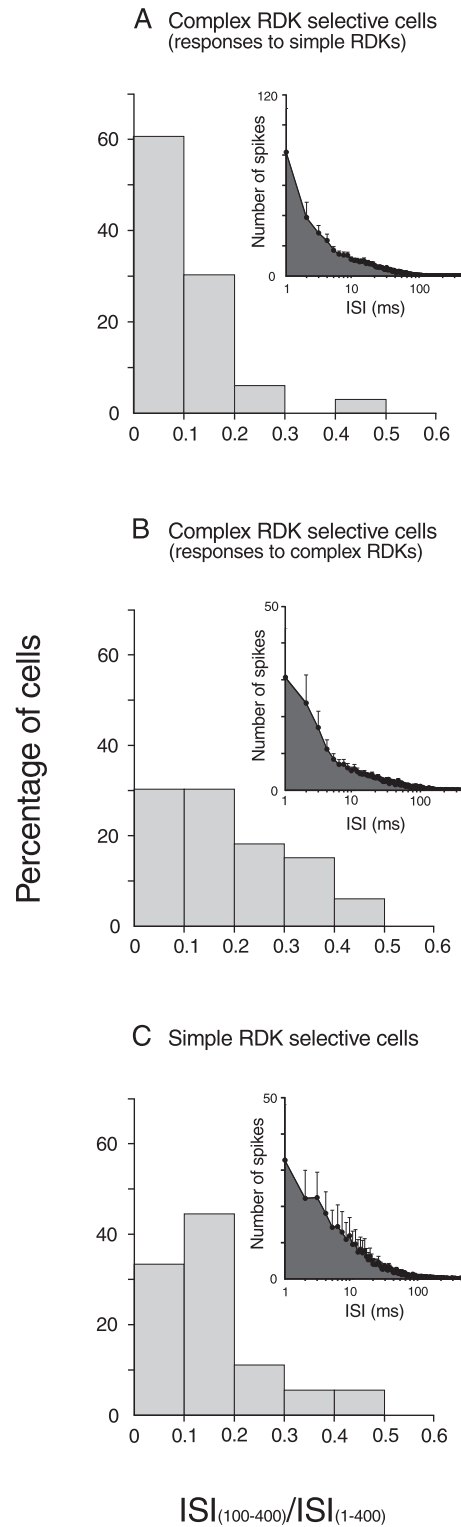


FIG. 5. Response profile to RDKs illustrated by the distribution of the $ISI_{100-400}/ISI_{(1-400)}$. Complex RDK-selective neurons. (A and B) Ratios computed from responses to complex and simple RDKs, respectively. (C) Ratios calculated from responses to simple RDKs. Insets depict the mean number of spikes (and SEM) for each ISI up to 400 ms (1-ms resolution). Two-way sample Kolmogorov–Smirnov indicates that the distributions of ISIs in panels A and B are significantly different. This observation stands when comparing distributions in panels A and C.

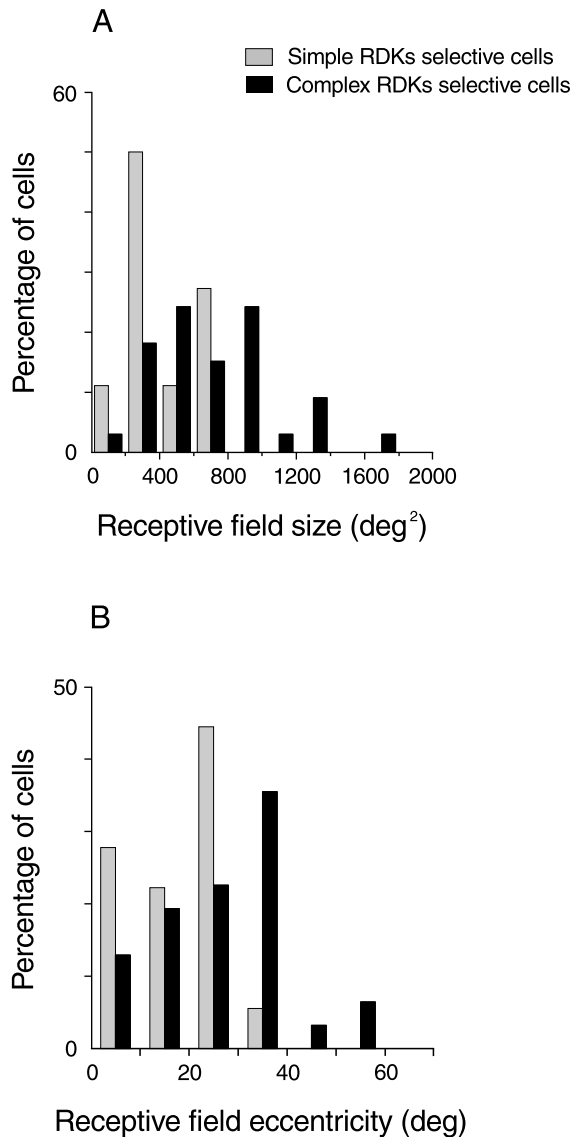


FIG. 6. Distribution of (A) receptive field size and (B) eccentricity for simple and complex RDK-selective units.

Influence of stimulus size

We investigated whether LP-pulvinar cells can discriminate the direction of complex RDKs when the latter was restricted to within the boundaries of their receptive fields. It was noted that units with large receptive fields (nine cells, mean area of 779 ± 151 square degrees) retained their ability to discriminate the global motion direction. A representative example is shown in Fig. 7. Panel A illustrates the responses of an LP-pulvinar neuron when most of the cat's visual field (full-screen stimulus) was stimulated with simple and complex RDKs. For both stimuli, the unit exhibited a clear preference for a specific range of motion (DIs), but the response to complex RDKs was more robust than that to simple RDKs. Fig. 7B shows the response of the same cell while the patterns were confined to its receptive field. Despite a small difference in the preferred direction (30° , which corresponds to the increment used to study direction selectivity), the response strength and selectivity (DI) was

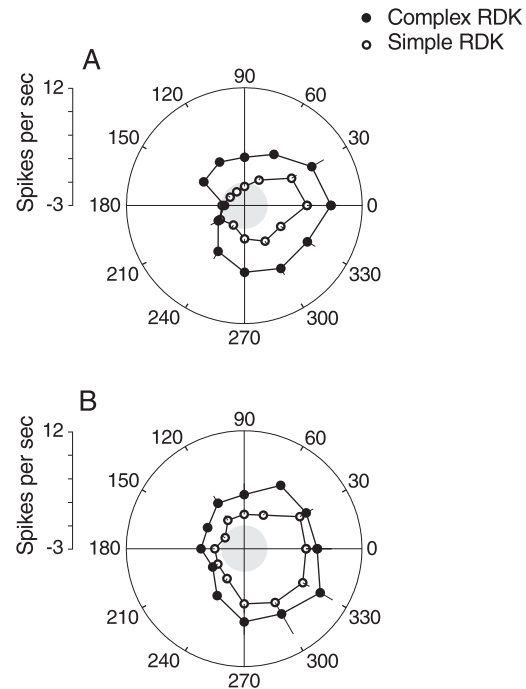


FIG. 7. Effects of restricting the patterns' dimension to receptive field size. (A) Responses to full-screen simple and complex RDKs. (B) Discharges of the same cell when both stimuli only covered the receptive field. One may note that the LP-pulvinar neuron can signal the true direction of motion of complex RDKs in both conditions. Conventions are as in Fig. 3.

comparable to the full-screen condition. The other five neurons had smaller receptive fields (mean 424 ± 88 square degrees) and when the pattern was restricted to the receptive field these units could still be driven by a complex RDK but the response profile was altered because their direction selectivity was reduced. Direction selectivity for simple RDKs was unaffected.

Influence of spatial and temporal intervals

The spatial interval between partner dots (D) yielding the optimal cell responses for complex RDKs was determined for 20 cells. Preferred spatial intervals were mainly distributed between 0.7 and 6.51° of visual angle and the mean value was $2.82 \pm 0.33^\circ$. The optimal spatial interval increased with receptive field size ($r = 0.53$, $P = 0.014$). The largest spatial interval (D_{\max}) for which LP-pulvinar cells could code the direction of complex RDKs (the temporal interval being constant) ranged between 2.18 and 10.66° (mean D_{\max} of $6.63 \pm 1.04^\circ$). Examples of the responses of two neurons as a function of D are presented in Fig. 8. These two units differed in their receptive field size (see insets). Figure 8A shows a cell that exhibited maximal directional preference for a D of 3° . For D -values $> 3^\circ$, direction selectivity was greatly reduced and, overall, responses became less robust for the largest D -value tested. Figure 8B depicts the responses of another LP-pulvinar cell with a smaller receptive field than in Panel A. Direction selectivity was roughly constant for low D -values but was almost abolished for a D of 2.8° . There appears to be a close relationship between receptive field size and optimal D -values (Fig. 8C), such that large LP-pulvinar receptive fields can code the direction of motion of global RDKs whose elements are separated by large distances.

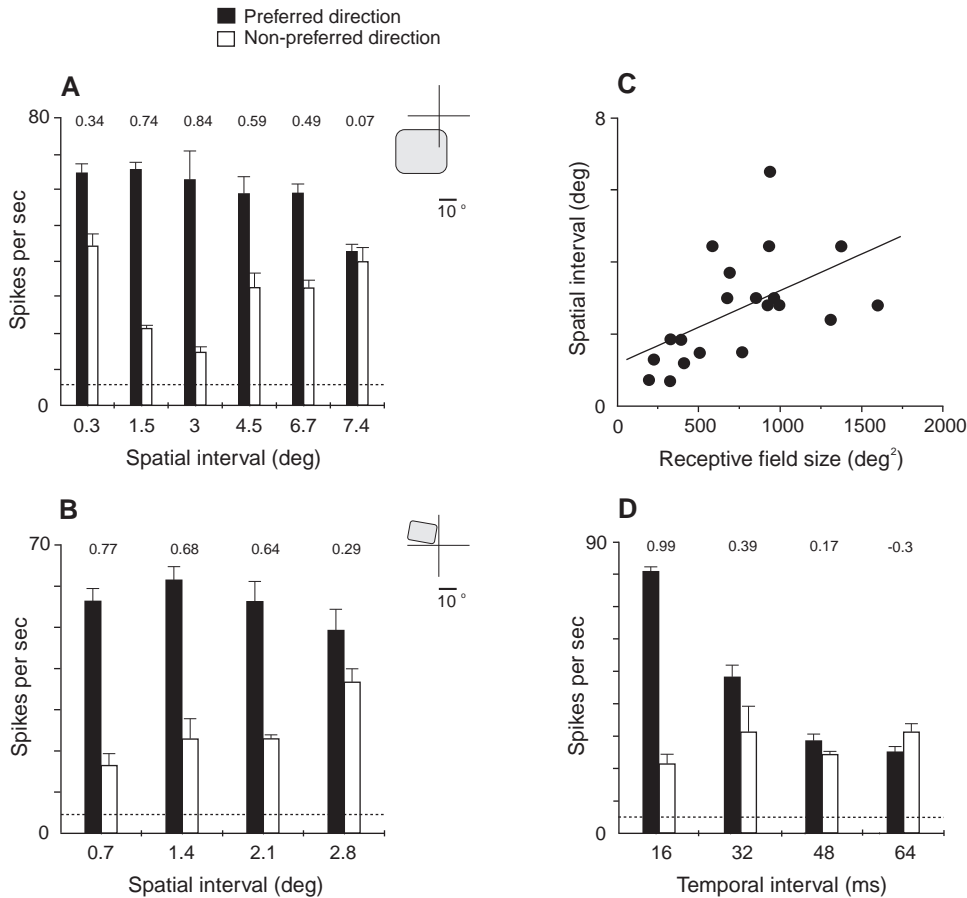


FIG. 8. (A and B) Influence of spatial interval between partner dots on response strength and direction selectivity. The large LP-pulvinar receptive field in A could signal the motion of complex RDKs whose comprising elements were separated by large spatial distances. The smaller receptive field shown in B coded much shorter displacements. Insets illustrate receptive field location and size (765 and 195 square degrees in A and B, respectively). (C) Correlation between receptive field size and preferred spatial interval of all LP-pulvinar cells ($r = 0.53$, $P = 0.014$). (D) Influence of temporal interval between partner dots. The direction selectivity and discharge rate of the LP-pulvinar neuron to the complex RDK were strongly reduced for intervals >16 ms. In A–C, the dashed lines represent spontaneous activity levels. Numbers on top of bar graphs represent direction index values. Error bars are SEM.

We also examined the responses of 11 cells when varying the temporal interval (T) between the appearances of given partner dots, i.e. the duration of the single *phi* motion jump (computed between the extinction of the dot at its initial spatial position and the appearance of the dot at its new spatial location). For all units, optimal responses were obtained for short temporal intervals (≈ 16 ms). A representative example is shown in Fig. 8D, where the response of a cell to both directions of motion is presented as a function of increasing T -values. Direction selectivity and response strength were markedly reduced at T -values >32 ms.

Relationship with pattern-motion selective units

Given that some neurons in the LP-pulvinar complex can signal the veridical direction of drifting plaid patterns, we investigated for a subset of 21 cells whether global and pattern-motion selectivity were coupled. Results are presented in Fig. 9. Most complex RDK-selective units (8 out of 14) were ‘unclassified direction-selective’ cells for plaids, i.e. they could not be categorized, on the basis of the calculation of partial correlation coefficients (see Materials and methods), in either the pattern- or component-motion categories. Five units were component-motion

selective and one was found to be pattern-motion selective. Similarly, the seven simple RDK-sensitive units tested were either component-motion selective, unclassified direction-selective or, in one case, pattern-motion selective. These data suggest that there is no strong relationship between RDK-defined global- and plaid-defined pattern-motion selectivity.

Cell localization

The position of 28 of 33 complex RDK-sensitive cells and 15 of 18 simple RDK units was assessed. In both cases, most of the units were located in the LPI or striate-recipient zone. Twenty-one complex RDK-sensitive units were located in the LPI and the remaining seven cells were located in the LPm. We found in each subdivision a pattern motion-selective neuron. Eleven simple RDK-selective cells were located in the LPI and four were found in the LPm.

Discussion

The results of this study indicate that a subpopulation of direction-selective cells in the cat’s LP-pulvinar complex can signal the true

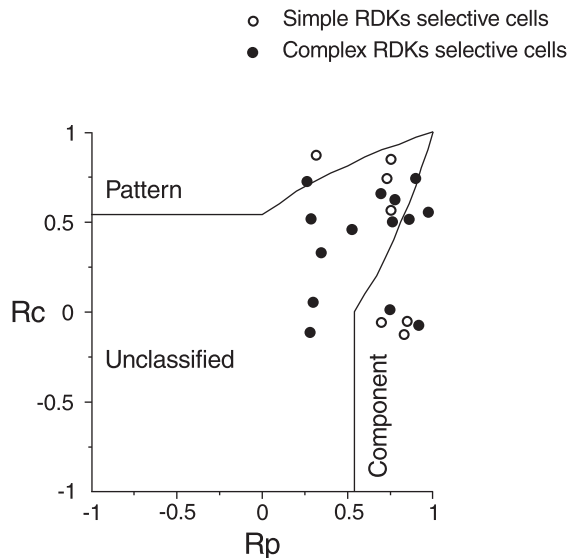


FIG. 9. Scatter plot in which the partial correlation for pattern and component selectivity of simple (open circles) and complex (filled circles) RDK-selective neurons are plotted against each other. The data space is divided into three statistical regions. Cells falling in the upper left and lower right areas are, respectively, pattern- and component-motion selective. The points lying in between represent unclassified direction-selective cells.

direction of a complex stimulus that requires the integration of local motion signals over space and time. These neurons differ from those only responding to simple RDKs by their receptive field size and eccentricity, and by their response profile. This finding represents the first evidence that global motion processing takes place in subcortical structures, and provides further support for the notion that LP-pulvinar neurons are involved in higher-order visual processing (Merabet *et al.*, 1998) which had only been attributed to cortical areas beyond the primary visual cortex in previous conceptualizations of motion processing (Movshon *et al.*, 1985; Newsome & Paré, 1988; Nowlan & Sejnowski, 1995; Scannel *et al.*, 1996).

In agreement with the notion that a large visual area of integration is necessary for global motion processing (Downing & Movshon, 1989), it was observed that the spatial extent of the receptive field of complex RDK-selective cells was significantly greater than that of simple RDK-selective units. In addition, our data revealed that the area of the large LP-pulvinar receptive fields is sufficient to integrate local motion cues in a coherent and global direction of motion. This capacity to adequately signal the global motion direction within the receptive field was less pronounced for receptive fields of a smaller size. Nonetheless, these same neurons were able to code the global motion direction of a full-screen pattern. It is therefore likely that, for small LP-pulvinar receptive fields, the analysis of global motion requires the recruitment of neighbouring cells to integrate motion information over an area larger than that of the classical receptive field. Of fundamental importance is the fact that LP-pulvinar neurons can code the displacement of elements in complex RDKs for large distances. Indeed, the D_{\max} was as high as 8° . This long-range spatial process occurred for short temporal intervals between the appearance of the two elements and, further, was positively correlated with receptive field size. These findings are comparable to those obtained in area MT of primates. By systematically varying the distance and time interval between successive stimuli in apparent motion displays, Mikami *et al.* (1986) found that MT neurons can detect directional

differences over spatial intervals that were roughly three times larger than those perceived by neurons in the primary visual cortex, whilst the temporal limits were similar for both areas. They reported, as we did, that the maximum spatial interval was correlated with receptive field size. The finding that MT lesions reduced the monkey's ability to discriminate global motion direction for large spatial intervals (Newsome & Paré, 1988) further supported the Mikami *et al.* (1986) data.

Our data suggest that there is no strong correspondence between PM and complex RDK selectivity nor between CM and simple RDK selectivity. Figure 9 shows indeed that complex and simple RDK selective cells were found in the three statistically defined areas. In other words, neurons sensitive to complex RDKs were not systematically pattern-selective when tested with drifting plaids. (One has to be cautious here since this classification is based on statistical evaluation of plaid responses, and cells considered as unclassified may well be sensitive, to some extent, to pattern motion.) A similar observation can be made for simple RDK-selective neurons and CM selectivity. Because most successful recordings were made in the LPI despite many attempts to reach the LPM, where lie the majority of PM-selective neurons (Merabet *et al.*, 1998), it precludes us from making definite conclusions regarding the sensitivity of a given cell to plaids and RDKs, particularly with regards to PM selectivity. Nevertheless, the above observations suggests that the nature of the integration underlying responses to the two kinds of patterns may differ, despite the fact that nonlinear mechanisms are involved in both cases (Adelson & Movshon, 1982; Adelson & Bergen, 1985; Baker & Hess, 1998). The simple RDK condition requires that contiguous receptive fields correlate their activation in respect to one another, which can be represented by simple motion mechanisms such as Reichardt detectors or similar units (Adelson & Bergen, 1985). On the other hand, simultaneous integration of single event *phi* motion over an area of the visual field (as was the case for complex RDKs), requires integration of higher order directional motion (Williams & Sekuler, 1984; Watamaniuk *et al.*, 1989). This inevitably involves another stage of analysis that integrates activation of receptive fields that are distant from one another (long-range processes). It is not surprising therefore that the receptive field sizes of cells that responded to complex motion were larger than the receptive field sizes of cells that responded primarily to simple motion cues. Although plaid motion also involves a nonlinear process like the complex motion task used here, it does not necessarily require long-range interactions. Rather, the process can be a second, non-Fourier (or rectification) stage, the likes of which have been proposed by Wilson *et al.* (1992). Thus, we propose that different cells are responsive to plaids than those sensitive to complex RDKs.

Functional considerations

This study provides additional evidence that the LP-pulvinar complex is part of neural networks involved in higher-order motion processing. Others and we previously suggested that cortico-thalamo-cortical loops involving the LP-pulvinar may be used, in part, to refine computations at cortical levels (Mumford, 1991; Miller, 1996; Merabet *et al.*, 1998). While little is known about the neural basis subtending global motion processing in the cat, there is some indication that the lateral suprasylvian (LS) cortex contributes to the latter. Rudolph & Pasternak (1996) reported that the destruction of the LS cortex impairs the capacity of the cat to discriminate the direction of global RDKs. In support of this, we recently found that a subset of direction-selective neurons in the posteromedial part of the LS (PMLS) cortex, but not in the striate cortex (see Fig. 3F), can code the direction of complex RDKs identical to that used in the present

study (preliminary data, not shown). Therefore, the LP-pulvinar neurons are likely to process global motion in close relationship with PMLS cortex. Interestingly this putative loop would be distinct from that described on the basis of plaid pattern selectivity. Pattern-selective cells were mainly located in the LPm (Merabet *et al.*, 1998), which is reciprocally linked to the AEV cortex (Mucke *et al.*, 1982), which is the only known cortical area in cats that contains such neurons. Complex RDK-sensitive units that establish connections with the PMLS cortex were found in the LPI (Abramson & Chalupa, 1985). The fact that complex RDK motion-sensitive units are not systematically clearly pattern motion-selective may indicate that the LP-pulvinar is not part of a circuit processing complex motion in general, but is rather directly involved in specific calculations carried out by different cortical modules subsuming different aspects of motion processing.

Acknowledgements

This work was supported by a CIHR grant (# MT-14825) to C.C. We thank A. Herbert and I. Ohzawa for commenting on a draft of the manuscript and F. Huppé-Gourgues and M. Villeneuve for providing help in some experiments. We also thank J.A. Movshon for providing the analysis software for the classification of plaid responses. FRSQ provided most of C.C.'s salary. (Chercheur boursier program), CIHR provided J.F.'s salary (investigator program) and D.D. was supported in part by an FCAR fellowship. Part of the visual software development (complex RDKs) was financially supported by a grant from the Réseau FRSQ de recherche en santé de la vision to C.C. and J.F.

Abbreviations

AChE, acetylcholinesterase; AEV, anterior ectosylvian visual; CM, component motion; D , spatial interval between partner dots; DI, direction selectivity index; D_{\max} , maximum displacement within which a cell still preferred a direction of motion of the pattern; ISI, interspike interval; LPI, lateral zone of the LP; LPm, medial zone of the LP; LP-pulvinar, lateral posterior-pulvinar; LS, lateral suprasylvian; MRC, mean response to complex RDKs at optimal direction; MRS, mean response to simple RDKs at optimal direction; MT, middle temporal; PM, pattern motion; PMLS, posteromedial part of the LS; PSTH, peristimulus time histogram; RDK, random-dot kinematogram; T , temporal interval between the appearances of given partner dots.

References

Abramson, B.P. & Chalupa, L.M. (1985) The laminar distribution of cortical connections with the tecto- and cortico-recipient zones in the cat's lateral posterior nucleus. *Neuroscience*, **15**, 81–95.

Adelson, E.H. & Bergen, J.R. (1985) Spatiotemporal energy models for the perception of motion. *J. Opt. Soc. Am. [A]*, **2**, 284–299.

Adelson, E.H. & Movshon, J.A. (1982) Phenomenal coherence of moving visual patterns. *Nature*, **300**, 523–525.

Baker, C.L. Jr & Hess, R.F. (1998) Two mechanisms underlie processing of stochastic motion stimuli. *Vision Res.*, **38**, 1211–1222.

Casanova, C., Freeman, R.D. & Nordmann, J.P. (1989) Monocular and binocular response properties of cells in the striate-recipient zone of the cat's lateral posterior-pulvinar complex. *J. Neurophysiol.*, **62**, 544–557.

Casanova, C., Savard, T., Nordmann, J.P., Molotchnikoff, S. & Minville, K.

(1995) Comparison of the responses to moving texture patterns of simple and complex cells in the cat's area 17. *J. Neurophysiol.*, **74**, 1271–1286.

Chalupa, L.M. & Abramson, B.P. (1989) Visual receptive fields in the striate-recipient zone of the lateral posterior-pulvinar complex. *J. Neurosci.*, **9**, 347–357.

Chalupa, L.M., Williams, R.W. & Hughes, M.J. (1983) Visual response properties in the tectorecipient zone of the cat's lateral posterior-pulvinar complex: a comparison with the superior colliculus. *J. Neurosci.*, **3**, 2587–2596.

Downing, C.J. & Movshon, J.A. (1989) Spatial and temporal summation in the detection of motion in stochastic random dot display. *Invest. Ophthalmol. Visual Sci. Supplement*, **30**, 72.

Graybiel, A.M. & Berson, D.M. (1980) Histochemical identification and afferent connections of subdivisions in the lateralis posterior-pulvinar complex and related thalamic nuclei in the cat. *Neuroscience*, **5**, 1175–1238.

Koelle, G.G. & Fridenwald, J.S. (1949) A histochemical method for localizing cholinesterase activity. *Proc. Soc. Exp. Biol. Med.*, **70**, 617–622.

Merabet, L., Desautels, A., Minville, K. & Casanova, C. (1998) Motion integration in a thalamic visual nucleus. *Nature*, **396**, 265–268.

Merabet, L., Minville, K., Ptito, M. & Casanova, C. (2000) Responses of neurons in the cat posteromedial lateral suprasylvian cortex to moving texture patterns. *Neuroscience*, **97**, 611–623.

Mikami, A., Newsome, W.T. & Wurtz, R.H. (1986) Motion selectivity in macaque visual cortex. II. Spatiotemporal range of directional interactions in MT and V1. *J. Neurophysiol.*, **55**, 1328–1339.

Miller, R. (1996) Cortico-thalamic interplay and the security of operation of neural assemblies and temporal chains in the cerebral cortex. *Biol. Cybern.*, **75**, 263–275.

Movshon, J.A., Adelson, E.H., Gizzi, M.S. & Newsome, W.T. (1985) The analysis of moving visual patterns. *Pont. Acad. Sci. Scr. Varia*, **54**, 117–151.

Mucke, L., Norita, M., Benedek, G. & Creutzfeldt, O. (1982) Physiologic and anatomic investigation of a visual cortical area situated in the ventral bank of the anterior ectosylvian sulcus of the cat. *Exp Brain Res.*, **46**, 1–11.

Mumford, D. (1991) On the computational architecture of the neocortex. I. The role of the thalamo-cortical loop. *Biol. Cybern.*, **65**, 135–145.

Newsome, W.T. & Paré, E.B. (1988) A selective impairment of motion perception following lesions of the middle temporal visual area (MT). *J. Neurosci.*, **8**, 2201–2211.

Nowlan, S.J. & Sejnowski, T.J. (1995) A selection model for motion processing in area MT of primates. *J. Neurosci.*, **15**, 1195–1214.

Rodman, H.R. & Albright, T.D. (1989) Single-unit analysis of pattern-motion selective properties in the middle temporal visual area (MT). *Exp. Brain Res.*, **75**, 53–64.

Rudolph, K.K. & Pasternak, T. (1996) Lesions in cat lateral suprasylvian cortex affect the perception of complex motion. *Cerebral Cortex*, **6**, 814–822.

Scannell, J.W., Sengpiel, F., Tovee, M.J., Benson, P.J., Blakemore, C. & Young, M.P. (1996) Visual motion processing in the anterior ectosylvian sulcus of the cat. *J. Neurophysiol.*, **76**, 895–907.

Sherman, S.M. & Guillery, R.W. (1996) Functional organization of thalamocortical relays. *J. Neurophysiol.*, **76**, 1367–1395.

Stoner, G.R. & Albright, T.D. (1992) Neural correlates of perceptual motion coherence. *Nature*, **358**, 412–414.

Watamaniuk, S.N., Sekuler, R. & Williams, D.W. (1989) Direction perception in complex dynamic displays: the integration of direction information. *Vision Res.*, **29**, 47–59.

Williams, D.W. & Sekuler, R. (1984) Coherent global motion percepts from stochastic local motions. *Vision Res.*, **24**, 55–62.

Wilson, H.R., Ferrera, V.P. & Yo, C. (1992) A psychophysically motivated model for the two-dimensional motion perception. *Visual Neurosci.*, **9**, 79–97.